



# Magnetic Properties of $x\text{CeO}_2 \cdot (50 - x)\text{PbO} \cdot 50\text{B}_2\text{O}_3$ Glasses and Glass Ceramics

G.El- Damrawi, F.Gharghar

Glass Research Group, Physics Department, Faculty of Science  
Mansoura University, 35516 Mansoura, Egypt

## Abstract

Cerium oxide in borate glasses of composition  $x\text{CeO}_2 \cdot (50 - x)\text{PbO} \cdot 50\text{B}_2\text{O}_3$  plays an important role in changing both microstructure and magnetic behaviors of the system. The structural role of  $\text{CeO}_2$  as an effective agent for cluster and crystal formation in borate network is clearly evidenced by XRD technique. Both structure and size of well-formed cerium separated clusters have an effective influence on the structural properties. The cluster aggregations are documented to be found in different range ordered structures, intermediate and long range orders are the most structures in which cerium phases are involved. The nano-sized crystallized cerium species in lead borate phase are evidenced to have magnetic behavior. The criteria of building new specific borate phase enriched with cerium as ferrimagnetism has been found to keep the magnetization in large scale even at extremely high temperature. Treating the glass thermally or exposing it to an effective dose of ionized radiation is evidenced to have an essential change in magnetic properties. Thermal heat treatment for some of investigated materials is observed to play dual roles in the glass matrix. It can not only enhance alignment processes of the magnetic moment but also increases the capacity of the crystallite species in the magnetic phases. On the other hand, reverse processes are remarked under the effect of irradiation. The magnetization was found to be lowered, since several types of the trap centers which are regarded as defective states can be produced by effect of ionized radiation.

## 1. Introduction

Materials containing cerium nanoparticles have recently attracted more attention due to their potential use in a wide technical field of applications [1-4]. This is may be due to increasing the demand for larger permanent magnet industry. In such situation, cerium oxide is used rather than other primary rare earth elements (REEs) such as europium, terbium, neodymium, samarium, and dysprosium. Therefore, development of materials based on cerium oxide is necessary to put the technology based on its magnetism in a much better place. This is because magnetization of the materials made from cerium modified glasses would exist even at correspondingly higher temperatures. The high temperature magnetization is available feature necessary for modern applications which based on materials of excellent unique magnetic properties. In addition,  $\text{CeO}_2$  containing materials offers high mechanical strength, good thermal stability and high capacity of oxygen storage. These advantages would recommend the materials to successful and widespread use in a variety of applications. For instances, it can be used in magnetism, medicine, imaging, communications technology and data storage.

Previous reported studies have been done to clarify the magnetic behavior of  $\text{CeO}_2$  in oxide glasses. The net result of these studies [5-11] has been shown that cerium oxide has specific magnetic behavior at and even above room temperature. However, until now, there is still a lack in information which required for fully characterization of magnetic behavior of cerium oxide in glasses and glass ceramics. Therefore, this work is devoted to shed more light on effect of different parameters on changing network structure and magnetic properties of a series of lead borate glasses containing  $\text{CeO}_2$ . Effects of glass composition, thermal heat treatment and irradiation are the main external parameters to be studied. Glass composition should be extended to contain an extremely high concentration from  $\text{CeO}_2$ . In such situation, cerium is forced to normally exist in different valance states. Both trivalent  $\text{Ce}^{3+}$  and tetravalent  $\text{Ce}^{4+}$  states are the most to be exist. Transition between the two states is the main reason for creating magnetization [5].

## 2. Experimental details

### 2.1. Sample preparation

The glass samples have been prepared using a normal melting method over a wide range of cerium oxide concentrations varied from 2.5 to 50 mol%  $\text{CeO}_2$ . The desired amount of high purity chemical compounds: cerium oxide ( $\text{CeO}_2$ ) lead oxide ( $\text{PbO}$ ), and boric acid ( $\text{H}_3\text{BO}_3$ ) were well mixed together to obtain fine powder. The batch mixture was then transferred to an alumina crucible and fused in an electric furnace. The melting process was carried out at different temperatures ranging between 800 °C and 1450 °C depending on the glass compositions. The melt was stirred several times until a complete homogenization was obtained. Each melt was then poured on stainless steel plate and pressed by another plate to take the final shape.

### 2.2. Measurement techniques

#### 2.2.1. X-ray diffraction (XRD)

The amorphous or crystalline nature of the structure was observed by X- ray diffraction. XRD measurements were carried out on powdered samples at (Metallurgical Institute, El-Tebbeen- Helwan) using a Bruker D8 Advance



powder XRD system with a Cu K $\alpha$  radiation ( $\lambda$ CuK $\alpha$  = 0.1540600nm). The range of the diffraction angle ( $2\theta$ ) is changed from 4° to 70° using a dwell time of 0.4 seconds.

### 2.2.2. Scanning electron microscope (SEM)

Scanning electron microscopy is widely used to examine surface modifications and microstructure of specimens. The morphology of the sample has been observed (Scanning Electron Microscope unit, Mansura University) using a JEOL-JSM-6510 LV Model with a working accelerating voltage of 25 kV and an increasing size image up to 300.000X. During SEM measurements, an electron beam is focused on a spot volume of the specimen, resulting interaction of the beams with the surface of the sample. The scattered electrons including secondary electrons, Auger electrons and back scattered electrons which can be detected and provide information on surface morphology. The surface of the samples has been covered with a thin layer of gold before SEM measurement to withstand the environment inside the microscope.

### 2.2.3. Energy dispersive X-ray analysis (EDX)

The energy dispersive X-ray spectra (EDX) of the samples were also acquired during their scanning electron microscopic (SEM) measurement. EDX Spectroscopy is based on the detection of the emitting of X-rays by the elements of the sample as a result of the ejected inner shell electrons using a high energy electron beam. The EDX spectrum normally involves peaks corresponding to X-rays generated by emission from different energy-levels in different elements. The higher concentrated elements in the sample present the most intense peaks in the spectrum. This technique is widely used for the identification of the elemental composition present in the sample.

### 2.2.4. Heat treatment (HT)

The selected samples containing 10, 20, and 40 mol% CeO<sub>2</sub>, were heated in a muffle furnace (Heraeus KR170) controlled within  $\pm 2$  °C. The samples were heat-treated at temperatures 200 °C and 400 °C for treatment time interval 2 and 4 hours respectively. After heating, the glasses were then kept into the furnace and held at the temperature of heat treatment for the desired time before cooling normally at room temperature.

### 2.2.5. Irradiation procedure

Gamma irradiation was performed at (National Institute for Radiation Research and Technology, Cairo, Egypt). The Irradiation test was carried out at room temperature using a Fricke dosimeter with a <sup>60</sup>Co gamma cell (2000 Ci) as gamma ray source. Each glass sample was subjected to a maximum total dose of  $45 \times 10^4$  Gy (45 Mrad). The irradiated samples were kept at 0°C until they used in order to reduce the external recovery processes which usually take place due to the light and the high temperature.

### 2.2.6. Magnetization measurements (VSM)

In order to investigate the magnetic behavior of the studied glasses, we have measured the magnetization (M) dependent curves of the magnetic field (H) at different CeO<sub>2</sub> concentrations  $0 \leq x \leq 50$  mol%. The magnetic measurements were performed using a Lake Shore Vibrating Sample magnetometer (VSM 7403, Metallurgical Institute, El-Tebbeen- Helwan). The specimen was filled into a tube and then placed in an applied field parallel to the vibrating direction. The magnetic hysteresis (M-H) loop was observed in magnetic field range of (-20,000 - 20,000 G) at room temperature. The magnetization values were divided by the sample weight, to obtain the magnetic moment per gram or emu/g as magnetization unit.

## 3. Results and discussions

Ferrimagnetism is the dominant type of magnetic ordering characterizes the magnetic properties of glasses. Its magnetic structure is composed of two magnetic sublattices separated by oxygen. Then the exchange interactions are mediated by the oxygen anions. Consequently, in the studied glasses, the strongest indirect interactions is expected to take place as result in an antiparallel order of spins between the two sublattices of Ce<sup>3+</sup> and Ce<sup>4+</sup>. The magnetic moments of the trivalent Ce<sup>3+</sup> and tetravalent Ce<sup>4+</sup> are not equal and result in a net magnetic moment characterizes the studied glasses as ferrimagnetic materials.

In addition to saturation magnetization, ferrimagnetic materials are able to retain the memory of their magnetic properties when an applied field is removed. This behavior will trace out a loop known as a hysteresis loop which represents the relationship between the applied magnetic field H and magnetization M. Fig. 1 shows the room temperature magnetization represented by closed loops for some of selected samples with varying cerium oxide content (x=0,2.5,10,20,30, and 40 mol%).

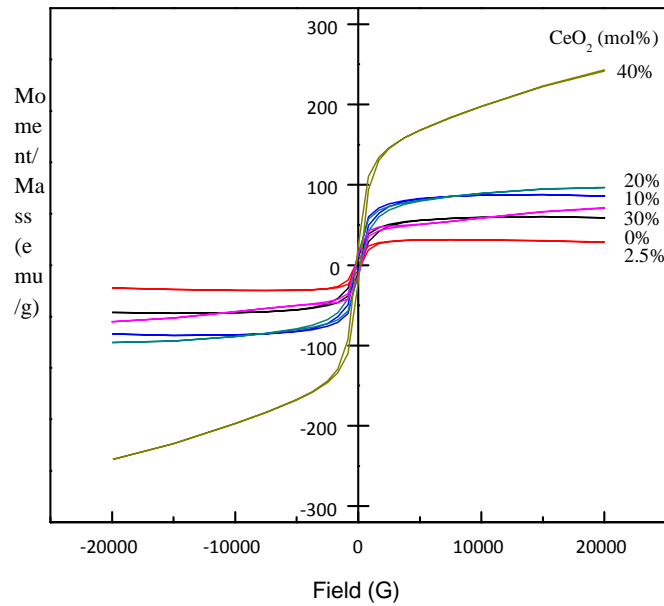


**Fig. 1: Room-temperature ferrimagnetic (RTFM) hysteresis curves for samples containing 0, 2.5, 10, 20, 30, and 40 mol% CeO<sub>2</sub>.**

The main glass matrix containing PbO and B<sub>2</sub>O<sub>3</sub> possesses a diamagnetic behavior [12, 13]. Substitution of cerium oxide with lead oxide in the host glass matrix is shown to have substantial change in magnetization of the tested materials. Fig. 2 presents dependence of saturation magnetic moment ( $M_s$ ) (in emu/g) on CeO<sub>2</sub> concentration. The  $M_s$  values show an increasing trend until ~ 20 mol% CeO<sub>2</sub> and then decreases until 35 mol% CeO<sub>2</sub>, then start to increase again with highest magnetization ( $M_s$  and  $A_t$ ) at 50 mol% CeO<sub>2</sub>. This behavior could be correlated to structural changes which occurred by the effect of CeO<sub>2</sub> substitution. Presence of crystallite species has the most predominant effect on the magnetic behavior of the glasses. It can be shown from fig. 2 that increasing of CeO<sub>2</sub> up to 20 mol% CeO<sub>2</sub> results in increasing magnetization. This increasing behavior is in a good correlation with result based on X-ray diffraction patterns of glasses containing the same concentration from CeO<sub>2</sub>. All X-Ray diffraction patterns (fig.3 left side) are showed to contain sharp peaks which are assigned to crystallized CeBO<sub>3</sub> [PDF nr.21-0177] and / or Ce(BO<sub>2</sub>)<sub>3</sub> [PDF nr.23-0877] species. Further increase in CeO<sub>2</sub>, leads to reduction in crystallinity and the network structure is mostly found in amorphous state. Consequently, their magnetization is decreased upon increasing CeO<sub>2</sub> concentration (Fig. 3 right side).

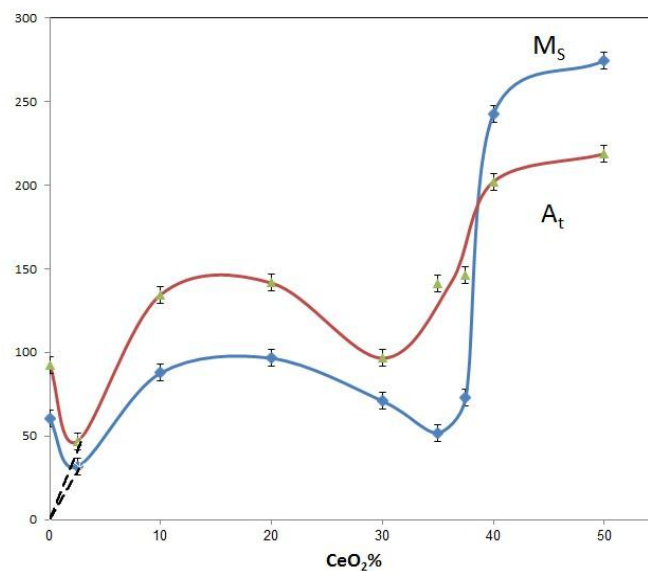


**Fig. 2: Saturation magnetization ( $M_s$ ) and total loop area ( $A_t$ ) of CeO<sub>2</sub>-PbO-B<sub>2</sub>O<sub>3</sub> as function of cerium oxide concentration.**

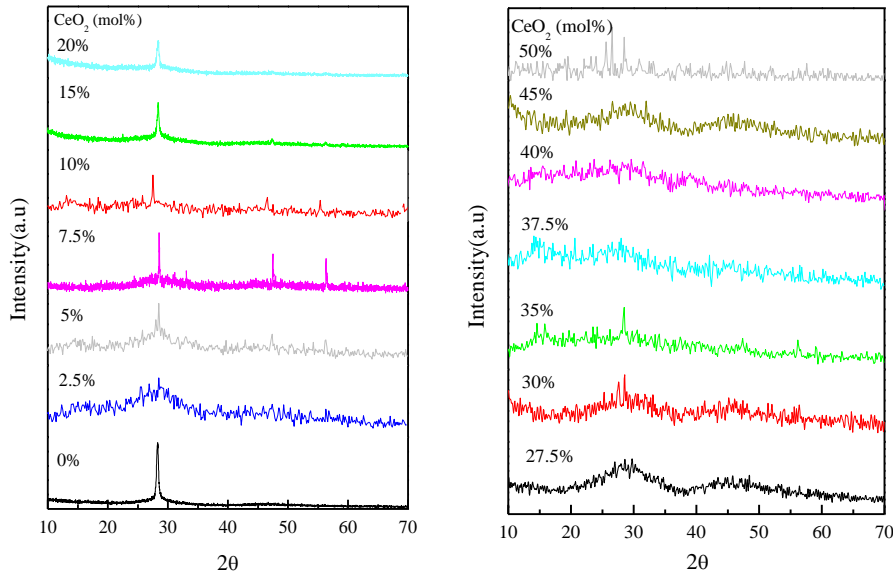


**Fig. 3: XRD of cerium lead borate glasses of different CeO<sub>2</sub> concentrations.**

Extra more addition of cerium oxide (37.5, 40, and 50 mol %) leads to increasing capacity of mixed valence of Ce<sup>3+</sup>/Ce<sup>4+</sup>. The transition from one oxide state to another plays the most important role in generating the magnetization in the samples at higher CeO<sub>2</sub> content. As a direct result, the magnetization showed a fast increasing trend in composition region  $\geq 37$  mol% CeO<sub>2</sub>. In such a case nano particles from crystalline cerium oxide as is evidenced from x-ray data are the most responsible for the large increase in magnetization.

As it mentioned above, cerium free PbO-B<sub>2</sub>O<sub>3</sub> glass possess a diamagnetism but in our case, the sample of 0 mol%CeO<sub>2</sub> exhibits RTFM as we can see in fig. 1 and fig. 2 with saturation magnetization M<sub>s</sub>=60.3emu/g. This value is even higher than that of sample containing of 2.5 mol% CeO<sub>2</sub> (M<sub>s</sub>=31.7emu/g). The magnetic impurities introduced from the starting materials, particularly CuO is considered to be responsible for inducing magnetization [14, 15] in PbO-B<sub>2</sub>O<sub>3</sub> glass. The elemental analyses of the sample free from CeO<sub>2</sub> have been tested by energy-dispersed X-ray spectrometry (EDX). The corresponding spectrum (Fig. 4) showed peaks related to copper element. Presence of copper even with limited concentration is expected to create magnetic signals and as a result, ferrimagnetism (FM) at 0% mol CeO<sub>2</sub> is evidenced to be present. The magnetization value of the 2.5 mol% CeO<sub>2</sub> is observed to be lower than possessed by glass of 0 mol% CeO<sub>2</sub>. The reduction in the magnetization is attributed to produce of competing magnetic interactions between nearby magnetic ions (Ce/Cu) which block or hinder each other. On the other hand, higher cerium oxide concentration leads to higher capacity of valence Ce<sup>3+</sup> and Ce<sup>4+</sup> ions which leads to higher magnetization. The effect of copper as impurity, in such case, is diluted by the effect of high content from cerium, since interaction between Ce<sup>3+</sup> and Ce<sup>4+</sup> is the more dominant.

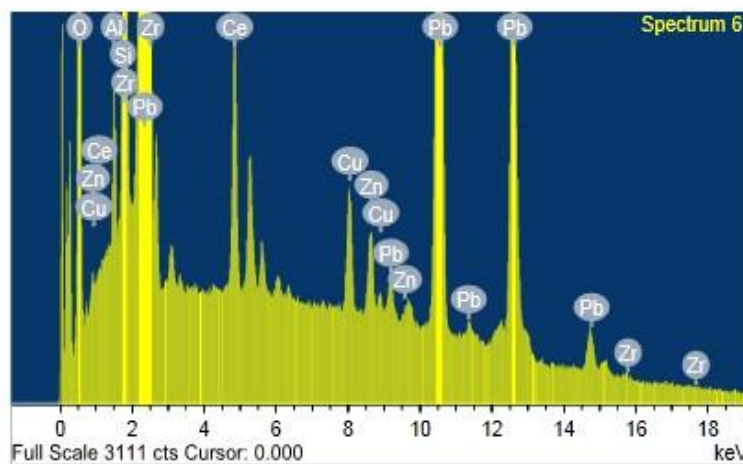


**Fig.4: Presence of all elements including the impurities in EDX image for 7.5 mol% CeO<sub>2</sub> sample**

### 3.1 Effect of thermal heat treatment

Fig. 5 shows the magnetization saturation of three selected samples containing 10, 20 and 40 mol% CeO<sub>2</sub> before and after heating at 200°C for 1h. As it can be notable, the saturation magnetization (M<sub>s</sub>) decreases with heating process for the three samples. It is obvious that the thermal treating process can't degrade magnetization of the material, only thermal heat treatment mainly affects the process of alignment between the magnetic spins. This effect is particularly due to increasing the random thermal vibrational motions which counteract the coupling forces between the adjacent atomic dipole moments [16]. As a result, some misalignments are produced between the magnetic dipoles. This effect can play the role of lowering the saturation magnetization in thermally treated glasses.

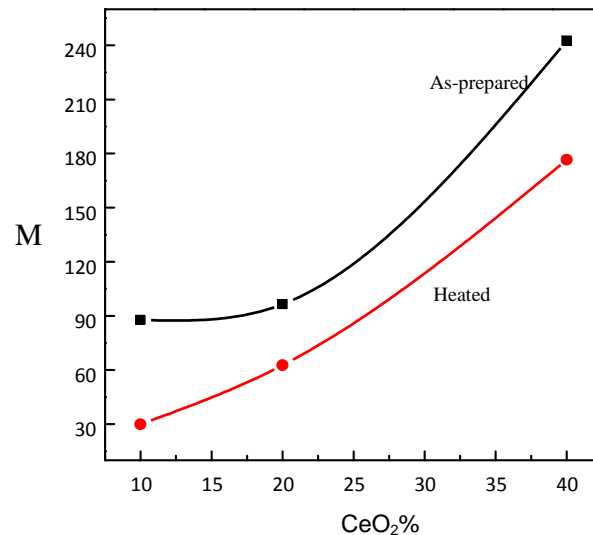


**Fig. 5: Saturation magnetism  $M_s$  as a function of CeO<sub>2</sub> content (10, 20, 40 mol %) for as-prepared and heated samples at 200°C for 1h.**

In general, heat treatment process can play a dual role [8, 12], it can lower the saturation limit of magnetization as in our case. In a severe case at extra higher temperatures it can destroy the mutual spin coupling forces [17] leading to losing the magnetic properties. On the other hand, it can produce phase separation and as a result, redistribution of ions or the molecules forming the glass network can take place. As a result, separated phases enriched with magnetic elements such as cerium can be constructed. In such situation, the magnetization is enhanced even at extremely high temperature as in our case.

As a further illustration, the above results were tested by treating the sample containing 20 mol% CeO<sub>2</sub> at higher temperature (400 °C) for 2h. In comparison, fig. 6 illustrates the variation of hysteresis curves and magnetic values for 20 mol% CeO<sub>2</sub> before and after heating at 200°C and 400 °C for 1 and 2h respectively. Both heat treated samples present similar behavior besides the measurements exhibit a little decay of magnetization with both heating temperatures comparing with the as-prepared sample. It is clear from the figure that, there is no any tendency toward demagnetization and the material keeps its magnetic behavior even at extra high temperature.

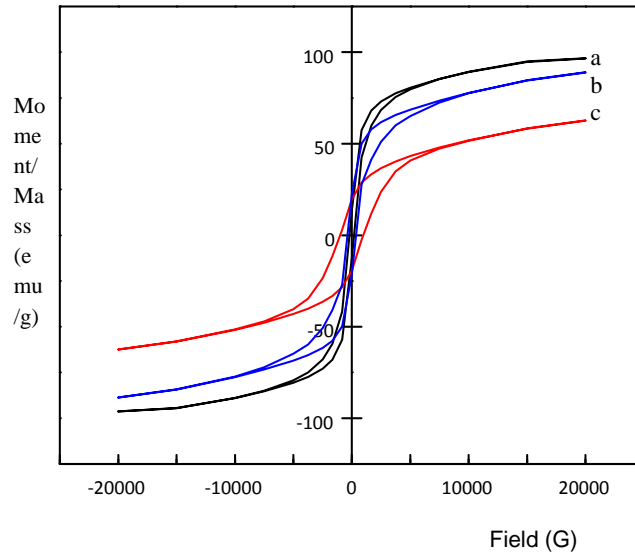


**Fig. 6: Room-temperature magnetic hysteresis curves of 20 mol% CeO<sub>2</sub> sample:**  
a- As-prepared,  $M_s=96.483$  emu/g, b- Heat treated (400 °C 2h),  $M_s=88.902$  emu/g, and c- Heat treated (200 °C 1h),  $M_s=62.666$  emu/g.

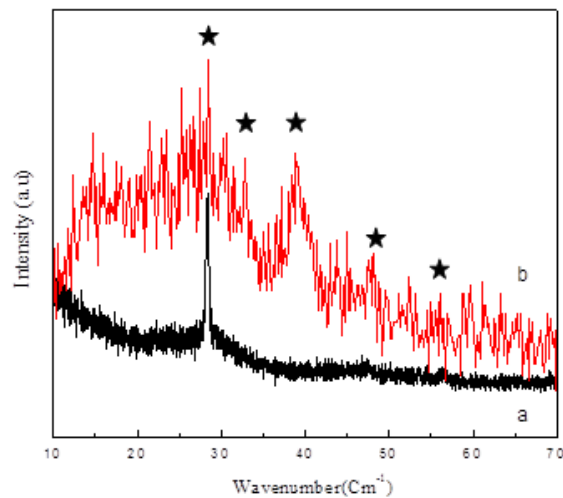


**Fig. 7: XRD of 20 mol% CeO<sub>2</sub> sample: a- As-prepared b- Heat treated (400°C, 2h).**

Furthermore, as can be noted, the heated sample at 400 °C has higher magnetic properties than the 200 °C one. This leads to conclude that HT process affected both crystallinity and moment arrangement as two important factors. One works on increasing magnetization and the other decreases it. Thus along with the base crystal phase [18], number of some separated phases enriched with cerium can be grown (see fig. 7), with increasing the heating temperature and time, which in turn withstand high temperature and increases the total magnetization. As a result, the saturated magnetization of sample treated at higher temperature and time is shown to offer high saturated magnetization.

### 3.2. Effect of irradiation on the magnetic properties

To study the effects of gamma irradiation on the studied glasses, two selected samples of concentration 10 and 20 mol% CeO<sub>2</sub> were irradiated at the same circumstances. For irradiated and un-irradiated samples, the magnetic behavior was measured and the obtained results are presented in fig. 8 and fig. 9. As it can be noted,  $M_s$  had particularly a sharp reduction by more than 60% upon irradiation for the sample containing 10 mol% CeO<sub>2</sub> since it decreased from 87.7 emu/g to 17.8 emu/g. Meanwhile, a less significant decrease is observed in the case of sample containing 20 mol% CeO<sub>2</sub> where  $M_s$  drops from 96.483 emu/g to 86.940 emu/g after irradiating. This observed changes can be associated with various types of defects produced by effect of ionized radiation [2, 19-22]. Some types of these defects are known to have a high ability to hinder the magnetic moment ordering and weakens the magnetic interaction in the samples. In this

regard, the matrix of the glass may suffer from damage due to the formation of aggregates which may be considered as point defects and dislocation during irradiation. In this case, formation of precipitates from boron rich in cerium is favored by effect of irradiation. Both processes result in an increase in the number of obstacles for dislocation movement, which in turn causes dominant damage process. However, the reduction of  $M_s$  is related with the stable matrix defect (SMD) due to the formation of agglomerates containing defects and dislocation loops during the irradiation. The distribution of nano-precipitates is expected to hinder the movement of magnetic domain introducing barriers on their path throughout the material [23]. Also, due to the nucleation and growth process that occur during irradiation [24, 25], different distribution of nano-precipitates would be resulted and has negative effect on magnetization, see fig. 10.

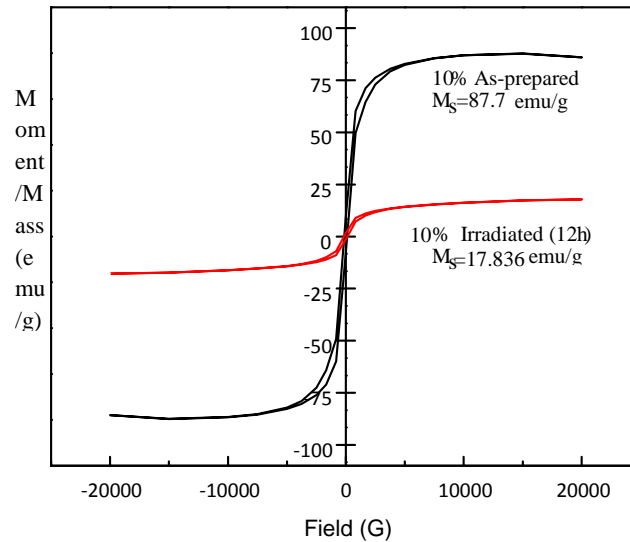


**Fig. 8: Room-temperature magnetic hysteresis curves of the as-prepared and irradiated samples for 10 mol% CeO<sub>2</sub>.**

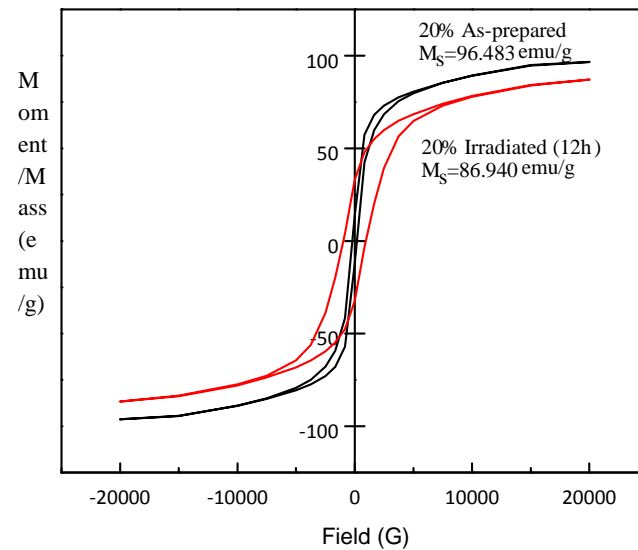


**Fig. 9: Room-temperature magnetic hysteresis curves of the as-prepared and irradiated samples for 20 mol% CeO<sub>2</sub>.**

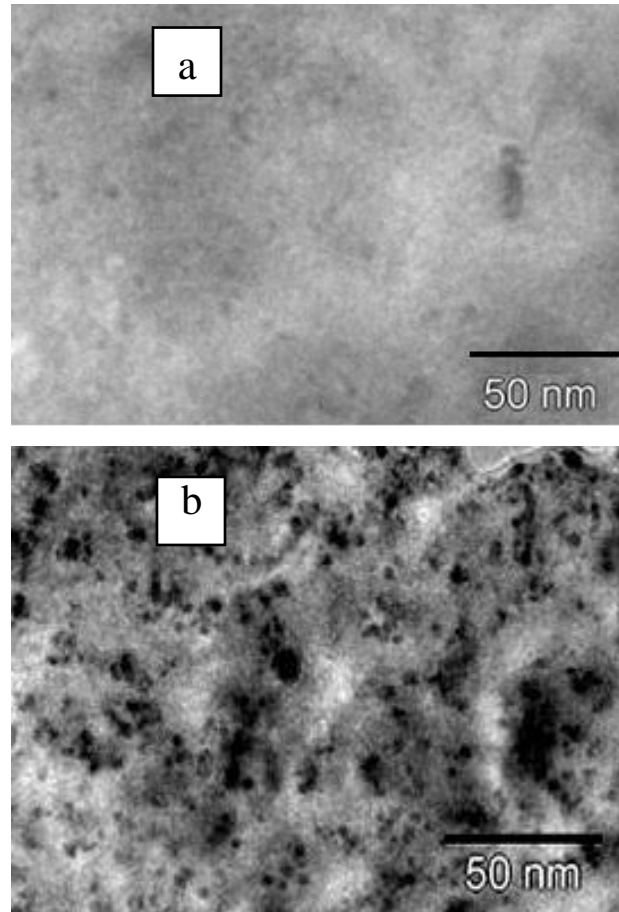


**Fig. 10: SEM analysis performed on 20 mol % CeO<sub>2</sub>: a- As-prepared, and b- Irradiated.**

#### 4. Conclusion

Cerium lead borate glasses exhibit ferrimagnetic (FM) behavior at and above room temperature. FM is very sensitive phenomena to many factors such as type and order of network structure (short, long and intermediate range orders), concentration of different oxidation states and also effect of the glass thermal history.

Magnetization is available in an extended large region of temperature, since the parameters determined magnetism all are presented in the corresponding hysteresis loops of the treated samples even at high temperature. The irradiation and heating process have different influence on the glass structure and consequently on magnetic behaviors. Thermal heat treatment can play a dual role, decreasing  $M_s$  or increasing it. While irradiation plays the role of creation of several types of defects, bonds damaging, and formation of aggregates. Therefore the irradiated sample showed precipitates in the range of nanometer which couldn't be observed in non-irradiated sample. The well-formed precipitates increase material deformation defects which are responsible for the reduction of  $M_s$  in irradiated materials.

#### References

- 1 Jha, A.R. 2014. Rare earth materials: properties and applications. CRC Press.
- 2 Marzouk, S.Y., Ezz-Eldin, F.M. 2008 Optical study of Ce<sup>3+</sup> ion in gamma-irradiated binary barium-borate glasses. *Physica B: Condensed Matter*. 403 (2008) 3307-15
- 3 Zu, C.K., Chen, J., Zhao, H.F., Han, B., Liu, Y.H., Wang, Y.H. 2009. Effect of cerium on luminescence and irradiation resistance of Tb<sup>3+</sup> doped silicate glasses. *Journal of Alloys and Compounds*. 479 (2009) 294-8.
- 4 Culea, E., Pop, L., Bosca, M. 2010 Structural and physical characteristics of CeO<sub>2</sub>-GeO<sub>2</sub>-PbO glasses and glass ceramics. *Journal of Alloys and Compounds*, 505 (2010) 754-7
- 5 Dutta, P., Pal, S., Seehra, M.S., Shi, Y., Eyring, E.M., Ernst. R.D. 2006. Concentration of Ce<sup>3+</sup> and oxygen vacancies in cerium oxide nanoparticles. *Chemistry of Materials* 18 (2006) 5144-6.
- 6 Ying-Zi, P., Yuan, L., Ru, B., De-Xuan, H., Zheng-Hong, Q. 2014. Magnetic behaviors of cerium oxide-based thin films deposited using electrochemical method. *Chinese Physics B*. 23 (2014) 097503.





- 7 Chen, X., Li, G., Su, Y., Qiu, X., Li, L., Zou, Z. 2009. Synthesis and room-temperature ferromagnetism of CeO<sub>2</sub> nanocrystals with nonmagnetic Ca<sup>2+</sup> doping. *Nanotechnology*. 20 (2009) 115606.
- 8 Zhang, Li., Zhang, M., Feng, R., Liu, W. 2010. Synthesis, structural and magnetic properties of CeO<sub>2</sub> nanoparticles. *IET Micro & Nano Letters*. 5 (2010) 95-9.
- 9 Tran, F., Karsai, P., Blaha, P. 2014. Nonmagnetic and ferromagnetic fcc cerium studied with one-electron methods. *Physical Review B*. 89 (2014)155106.
- 10 Slusser, P.K. 2009. Transition Metal Doped Cerium Oxide for Spintronics Applications. Doctoral dissertation. University of Utah.
- 11 Ge, M.Y., Wang, H., Liu, E.Z., Liu, J.F., Jiang J.Z., Li, Y.K., Xu Z.A., Li, H.Y. 2008. On the origin of ferromagnetism in CeO<sub>2</sub> nanocubes. *Applied Physics Letters*. 93 (2008) 2505.
- 12 Burzo, E., Ardelean, I., Măţulescu, D. 1992. Magnetic properties of xCeO<sub>2</sub>(1- x) (3B<sub>2</sub>O<sub>3</sub>· PbO) glasses. *Journal of materials science letters*. 11 (1992) 1496-1497.
- 13 Ardelean, I., Ilonca, G., Bărbos, D. 1981. Magnetic properties of xCoO. (1- x)[2B<sub>2</sub>O<sub>3</sub>· PbO] glasses. *Solid State Communications*. 39 (1981) 1345-6.
- 14 Hammad, T.M., Salem, J.K., Harrison, R.G., Hempelmann, R., Hejazy, N. K. 2013. Optical and magnetic properties of Cu-doped ZnO nanoparticles. *Journal of Materials Science: Materials in Electronics*. 24 (2013) 2846-52.
- 15 Kastner, M.A., Birgeneau, R.J., Shirane, G., Endoh. Y. 1998. Magnetic, transport, and optical properties of monolayer copper oxides. *Reviews of Modern Physics*. 70 (1998) 897.
- 16 Dhannia, T., Jayalekshmi, S. 2012. Investigations on the structural, optical and Magnetic properties of nanostructured cerium oxide in pure and doped forms and its polymer nanocomposiets. PhD diss. Cochin University of Science and Technology.
- 17 Getachew, W. 2013. Parametrization of Ferromagnetic Phase Transition in Fe. Doctoral dissertation, Addis Ababa University.
- 18 El-Damrawi, G., Gharghar, F., Ramadan, R. M. 2016. Structural studies on new xCeO<sub>2</sub>·(50- x)PbO·50B<sub>2</sub>O<sub>3</sub> glasses and glass ceramics. *Journal of NonCrystalline Solids* 452(2016)291-6.
- 19 Allred, C. L. 2003. Effect of radiation on silicon and borosilicate glass. MASSACHUSETTS INST OF TECCAMBRIDGE.
- 20 Baccaro, S., Cemmi, A., Di Sarcina, I., Menchini, F. 2015. Gamma Rays Effects on the Optical Properties of Cerium Doped Glasses. *International Journal of Applied Glass Science*. 6 (2015) 295-301.
- 21 Doweidar, H., Zeid, M.A., El-Damrawy, G.M. 1991. Effect of gamma radiation and thermal treatment on some physical properties of ZnO-PbO-B<sub>2</sub>O<sub>3</sub> glasses. *Journal of Physics D: Applied Physics*. 24 (1991) 2222
- 22 Laopaiboon, R., Bootjomchai, C. 2014. Radiation effects on structural properties of glass by using ultrasonic techniques and FTIR spectroscopy: a comparison between local sand and SiO<sub>2</sub>. *Annals of Nuclear Energy*. 68 (2014) 220-7.
- 23 Leslie-Pelecky, D.L., Rieke. R.D. 1996. Magnetic properties of nanostructured materials. *Chemistry of materials*. 8 (1996) 1770-83.
- 24 De Lamaestre, R. E., Béa, H., Bernas, H., Belloni, J., Marignier, J.L. 2007. Irradiation-induced Ag nanocluster nucleation in silicate glasses: Analogy with photography. *Physical Review B*. 76 (2007) 205431.
- 25 Ye. B. 2011. Formation and growth of irradiation-induced defect structures in ceria. Doctoral dissertation. University of Illinois at Urbana-Champaign.